Separation Science and Technology
Publication details, including instructions for authors and subscription information:
http://www.informaworld.com/smpp/title~content=t713708471

Xylene Vapor Mixture Separation in Nanocomposite MFI-Alumina Tubular Membranes: Influence of Operating Variables

M. O. Daramola[a]; A. J. Burger[a]; M. Pera-Titus[b]; A. Giroir-Fendler[b]; L. Lorenzen[a]; J. -A. Dalmon[b]
[a] Department of Process Engineering, Stellenbosch University, Matieland, Stellenbosch, South Africa [b] University of Lyon, Institute of Research on the Catalysis and the Environment of Lyon (IRCELYON), Villeurbanne Cedex, France

Online publication date: 07 January 2010

To cite this Article Daramola, M. O. , Burger, A. J. , Pera-Titus, M. , Giroir-Fendler, A. , Lorenzen, L. and Dalmon, J. -A.(2010) 'Xylene Vapor Mixture Separation in Nanocomposite MFI-Alumina Tubular Membranes: Influence of Operating Variables', Separation Science and Technology, 45: 1, 21 — 27
To link to this Article: DOI: 10.1080/01496390903402141
URL: http://dx.doi.org/10.1080/01496390903402141

Separation Science and Technology, 45: 21–27, 2010

ISSN: 0149-6395 print/1520-5754 online
DOI: 10.1080/01496390903402141

Taylor & Francis
Taylor & Francis Group

Xylene Vapor Mixture Separation in Nanocomposite MFI-Alumina Tubular Membranes: Influence of Operating Variables

M. O. Daramola,[1] A. J. Burger,[1] M. Pera-Titus,[2] A. Giroir-Fendler,[2] L. Lorenzen,[1,‡] and J.-A. Dalmon[2]

[1]*Department of Process Engineering, Stellenbosch University, Matieland, Stellenbosch, South Africa*
[2]*University of Lyon, Institute of Research on the Catalysis and the Environment of Lyon (IRCELYON), Villeurbanne Cedex, France*

In this study, we present the results of a preliminary investigation on the influence of operating variables (temperature, sweep gas flow rate, and total feed vapor pressure) on xylene vapor mixture separation using tubular nanocomposite MFI-alumina zeolite membrane prepared by the pore-plugging synthesis technique. Within the detection limit of our analytical system, neither m- nor o-xylene was detected in the permeate stream, the membranes displaying therefore "infinite" p-xylene selectivity. The mixture's p-xylene flux displayed a maximum value of ca. 3.5 $\mu mol \cdot m^{-2} \cdot s^{-1}$, corresponding to a mixture permeance of 11 $nmol \cdot m^{-2} \cdot s^{-1} \cdot Pa^{-1}$, at 473 K and for a feed composition 0.63 kPa p-xylene/0.27 kPa m-xylene/0.32 kPa o-xylene, being almost unchanged for sweep gas flow rates (N_2) higher than 20 mL(STP)/min and increasing with the total xylene vapor pressure at 1 : 1 : 1–3 p/m/o-xylene composition. The experimental p-xylene fluxes can be well predicted by a Maxwell-Stefan model, as expected for a mass transfer process driven by competitive adsorption / surface diffusion. Unlike film-like MFI membranes, the membranes presented here preserved their selectivity to p-xylene for total xylene pressures as high as 150 kPa. This behavior is attributed to the intimate contact between the alumina confining pores and MFI nanoparticles, reducing long-term stresses and thus preventing distortion of the MFI framework during p-xylene adsorption. These results open up potential applications of nanocomposite MFI-alumina for selective p-xylene separations at high loadings, for instance in pervaporation, where the use of film-like MFI membranes is discouraged.

Keywords MFI; nanocomposite; separation; xylenes; zeolite membrane

INTRODUCTION

Xylenes are petrochemical intermediates industrially produced as a mixture of ortho, meta, and para isomers and ethylbenzene in the aromatic C8 cut. Xylenes are obtained either from high-severity catalytic reforming of naphtha or from the pyrolysis gasoline stream in a naphtha steam cracker. In 1999, the production value of mixed xylenes was estimated to about 5 billion US $, second only to benzene in aromatic production (1).

Amongst mixed xylenes, *p*-xylene is the most industrially valuable isomer, almost exclusively consumed in the production of teraphthalic acid (TPA) and dimethyl terephthalate (DMT), both used in the manufacture of polyethylene terephthalate (PET) for polyester fibers, films, and solid-state packaging resins. According to UK consultants Tecnon OrbiChem (2), global p-xylene markets have been tight through 2006 and 2007, with p-xylene utilization rates higher than 90%. Asian markets have been particularly tight with demand exceeding supply. The world p-xylene demand has been growing steadily in the last 5 years and this growing trend is expected to be pursued in the period 2008–2013 at an average estimated rate of 7%/year (8.5%/year in Asia).

The relevance of p-xylene as intermediate in the synthesis of polymers necessitates the development of processes for its separation and purification. Because of their similar physical properties, xylene isomers can hardly be separated by distillation (1,3,4). Currently, industry relies on fractional crystallization and preferential adsorption to separate xylene isomer mixtures. Both techniques are batch processes and energy-intensive, inflating therefore the production costs and their environmental impact. As a matter of example, the United States consumed nearly 100 quadrillion BTU in 2004, corresponding approximately to one fourth of the world's energy (5). Petrochemical and chemical industries accounted for 13 quadrillion BTUs in 1998 with about 35% of the energy consumption used in the

Received 16 April 2009; accepted 31 August 2009.

‡Current address: BHP Billiton SSM, Perth Technology Centre, Australia.

Address correspondence to M. O. Daramola, Department of Process Engineering, Stellenbosch University, Private Bag XI, Matieland, Stellenbosch 7602, South Africa. Tel.: 27218083860; Fax: 27218082059. E-mail: darmola@sun.ac.za; E-mail: marc.pera-titus@ircelyon.univ-lyon1.fr

manufacture and separation of organic chemicals (mainly for heating/cooling) (6). It seems therefore imperative to move to more energy-efficient and environmentally-friendly processes involving less heating/cooling steps (and operating in continuous mode) for p-xylene separation. Membrane technology constitutes a promising option to achieve this goal. As the driving force in a gas-separation membrane is the pressure difference between the feed/retentate and permeate, the heating/cooling costs can be dramatically reduced compared to more conventional separation processes (e.g., distillation, crystallization or adsorption). Furthermore, the combination of membrane separation with (reactive) distillation in hybrid separation processes (for instance for distillate/residue separation) can also help reducing cooling/heating costs and promote process intensification (see for instance refs (7,8)).

Because polymeric membranes (e.g., PVA) have not proven to be successful for xylene isomer separation, researchers have moved to zeolites and other molecular sieve membranes. Several recent studies have pointed out the potentials of MFI zeolite membranes for xylene separation and purification, either by pervaporation (PV) (9) or by vapor permeation (VP) (10–18). As the kinetic diameter of p-xylene (5.8 Å) is smaller than that of o- and m-xylene (6.8 Å each) and close to the pore size of the MFI channels (5.4×5.6 Å and 5.1×5.6 Å) (19), p-xylene is expected to diffuse faster within the MFI framework, allowing therefore its separation from a mixture of isomers. Moreover, the lower size and ordered packing of p-xylene promotes its adsorption in MFI channels, mainly driven by configurational entropy effects (20).

It is well known that the MFI framework can experience distortions induced by p-xylene adsorption (21–24). These distortions translate into phase changes, especially pronounced at near-ambient temperature and high p-xylene loadings, leading to channel "swelling" that renders the material unable to distinguish between the different xylene isomers. As a result, single-file diffusion may occur, xylene isomers not being able to diffuse one another in the zeolite channels. This implies that xylene isomers with the slowest permeation rate (i.e., o- and m-xylenes) might limit diffusion, blocking p-xylene separation and reducing therefore membrane selectivity. This strong limitation of MFI materials acts as a deterrent for the application of MFI membranes for xylene separation at high loadings, for instance in PV separations.

Nevertheless, at sufficiently low xylene partial pressures (<2 kPa) and in the temperature range 295–673 K, MFI membranes can show optimal selectivity for p-xylene separation by VP. By now, the best separation and permeation results have been obtained by Tsapatsis group (25) using "microstructurally optimized" b-oriented MFI films prepared by secondary growth hydrothermal synthesis using a b-oriented seed layer and trimer-TPA as a template in the secondary growth step. The membranes offer p-xylene permeances of about $200\,\mathrm{nmol \cdot m^{-2} \cdot s^{-1} \cdot Pa^{-1}}$ at 473 K for a feed mixture of 0.45 and 0.35 kPa p- and o-xylene, respectively, with p/o-xylene separation factors between 200–500. Our group has prepared highly reproducible tubular MFI membranes (26) and hollow fibers (27) displaying excellent xylene isomer vapor separation properties and p-xylene permeances about $10\,\mathrm{nmol \cdot m^{-2} \cdot s^{-1} \cdot Pa^{-1}}$ at 473 K. Compared to most commonly used film-like MFI membranes (either with preferential or random channel orientation), the membranes prepared here consist of randomly oriented MFI crystal nanocomposites grown inside an alumina porous matrix via a pore-plugging hydrothermal synthesis approach.

This paper reports additional mixture permeation data on xylene isomer separation using nanocomposite MFI-alumina tubular membranes, focusing specifically on the effect of the main operational variables (temperature, xylene vapor pressure, and sweep gas flow rate). Our goal is to show that, by confining the zeolite material, a nanocomposite MFI-alumina membrane can show high selectivity to p-xylene at high xylene loadings compared to more conventional film-like MFI membranes.

EXPERIMENTAL

Membrane Preparation and Quality Testing

The nanocomposite MFI-alumina membrane used in this study was prepared via pore-plugging *in situ* hydrothermal synthesis on an asymmetrical Pall-Exekia α-alumina tube (o.d. 10 mm, i.d. 7 mm, length 15 cm, active permeation area 26 $\mathrm{cm^2}$) as described elsewhere (28,29). The cross-sectional layers of the support has dimensions: outer layer, 12 μm; intermediate layer, 0.8 μm; inner layer, 0.2 μm. The nanocomposite nature of the fibers was inspected by SEM (JSM-5800LV, 20 kV) coupled with EDX analysis (Edax Phoenix, 1-μm microprobe).

The quality of the membrane was evaluated using single gas hydrogen permeation, binary mixture separation with *n*-butane/H_2 and by dynamic desorption of adsorbing species under cross membrane pressure difference on the guidance of a previous study (30). This method relies on the permeation of H_2 within a membrane, the intra- and intercrystalline pores having been previously pre-plugged with n-butane at 14 kPa partial pressure for 1 h. Before membrane quality testing, the membrane was mounted on the membrane module and subjected to high temperature pre-treatment at 673 K under a 20 mL(STP)/min N_2 flow on the retentate and permeate sides as described in a previous study (31) to remove the adsorbed moisture and other contaminants. This pre-treatment was also carried out before each series of xylene VP tests.

Membrane Separation

The set-up used for membrane separation has been described in a previous study (27). Ternary xylene mixtures (p-xylene, 99% purity; m-xylene, 99% purity; o-xylene, 97% purity) purchased from Sigma-Aldrich were saturated in dry N_2 at a 10-mL(STP)/min carrier flow at atmospheric pressure using two saturators combined in series. The first bubbler was kept at 323–393 K depending on the desired xylene partial pressure, while the second bubbler was maintained at a temperature of about 6 K lower to ensure saturation. The permeate side of the membrane was swept using N_2 at several flow rates in the range 5–30 mL (STP)/min. After attaining steady state in about 5 h, the composition of the feed, retentate, and permeate streams was analyzed online using a gas chromatograph (Shimadzu GC-14A) equipped with a solgel-WAX capillary column and a flame ionization detector (FID). To avoid any condensation and ensure proper xylene partial pressure throughout the system, all the lines were heated and maintained at 393 K using heating tapes. Xylene vapor separation and permeation experiments were performed in Wicke-Kallenbach mode to prevent occurrence of viscous flow. In all the experiments, mass balances of each xylene isomer were closed with an experimental error <15%.

The membrane performance was evaluated in terms of permeation flux (or xylene permeance), p/o and p/m xylene permselectivity (or ideal selectivity), and p/o and p/m mixture separation factor. The separation factor ($Sf_{i,j}$) was defined as the enrichment factor of one component to another in the permeate, as compared to the feed composition ratio (Eq. 1)

$$Sf_{i/j} = (y_i/y_j)_{permeate}/(x_i/x_j)_{feed} \quad (1)$$

where y is the mole fraction and in this case, i = p-xylene and j = o-, m-xylene.

RESULTS AND DISCUSSION

Membrane Quality

The membrane prepared in this study shows a room-temperature pure hydrogen permeance of 0.49 μmol.m^{-2}.s^{-1}.Pa^{-1} and a *n*-butane/H_2 separation factor as high as 100 after pre-treatment. This latter value reflects good membrane quality in terms of low amount of intercrystalline defects. The good membrane quality of the membrane prepared in this study can also be inferred from the extremely slow *n*-butane desorption dynamics under the presence of a transmembrane pressure of pure hydrogen at room temperature (see Fig. 1). The desorption dynamics is especially slow in the first 4 h, the membrane taking about 29 h to recover at least 90% of its original pure hydrogen permeance. As a matter of fact, in a standard desorption test, *n*-butane is expected to desorb faster from intercrystalline domains than from zeolite pores (intracrystalline), where adsorption forces are expected to be stronger. A slow desorption dynamics, especially at short times, is therefore an indicator of a low number of intercrystalline domains.

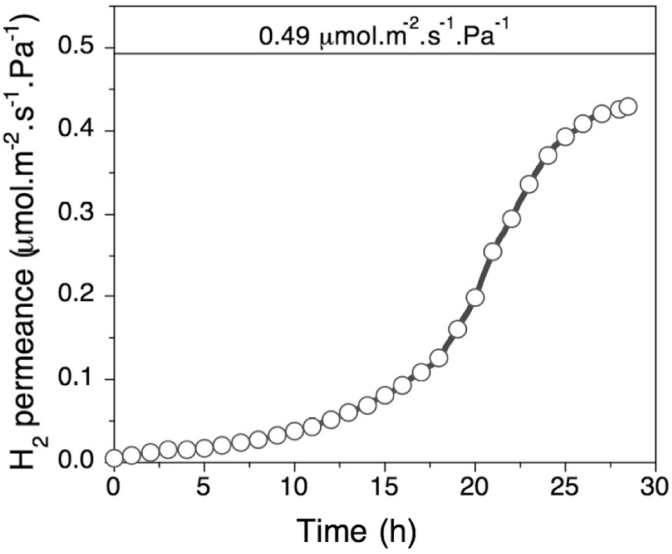

FIG. 1. Absolute hydrogen permeance as a function of time in a *n*-butane room-temperature desorption experiment (0.49 μmol · m^{-2} · s^{-1} · Pa^{-1} is the pure hydrogen permeance at room temperature).

Also, the SEM micrographs (see Fig. 2) confirm the formation of a nanocomposite material on the substrate, namely no continous MFI film is formed on top of the support. Also, Fig. 2 (top) shows good pore-plugging of the 0.2-μm layer with zeolite crystals. The EDX analyses show an average Si/A1ratio about 10–20 (semi-quantitative analysis) on the inner active layer. The material in the active layer corresponds accordingly to an Al-enriched H-ZSM-5 zeolite.

Xylene Vapor Permeation

Effect of Temperature

Figure 3 plots the evolution of the p-, m-, and o-xylene fluxes and p/o and p/m separation factors as a function of temperature in the range 400–700 K for the membrane prepared in this study. Since m-xylene and o-xylene signals in the permeate stream were below the detection limit of our GC, we have computed the p/o and p/m separation factors in such conditions (in practice 'infinite') from the minimum detectable o- an m-xylene partial pressures in the permeate (10^{-3} kPa for m-xylene and 10^{-4} kPa for o-xylene).

The p-xylene transmembrane flux shows a maximum value of 3.5 μmol.m^{-2}.s^{-1} at 473 K, corresponding to a permeance about 11 nmol · m^{-2} · s^{-1} · Pa^{-1}. As expected for a nanocomposite material (32), the p-xylene flux decreases monotonically after the maximum with no further increase

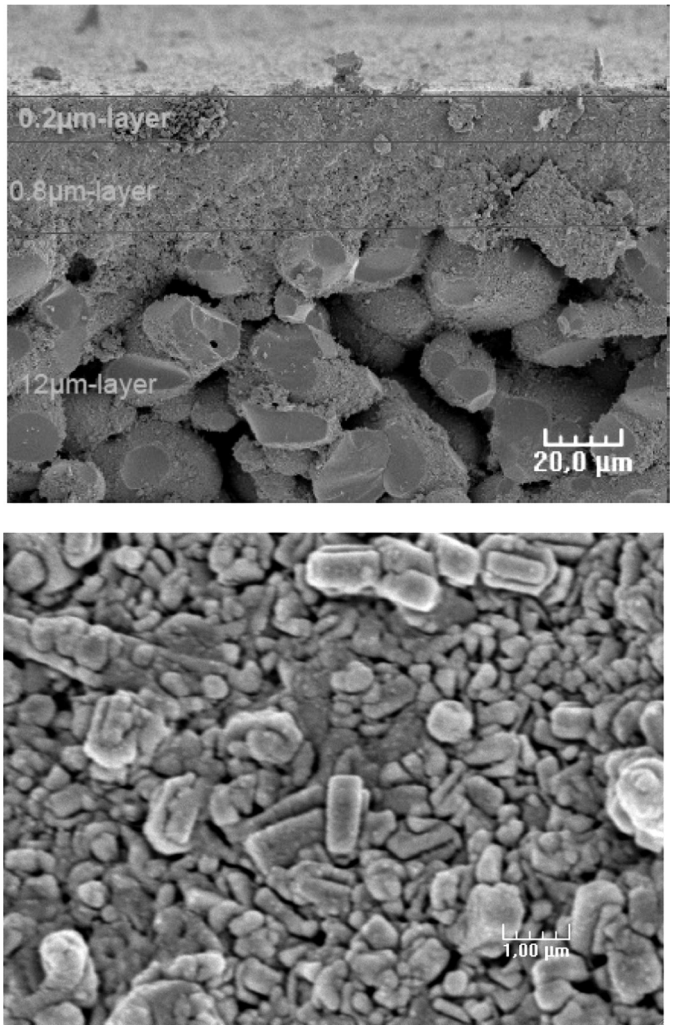

FIG. 2. SEM micrographs of the membrane showing formation of nanocomposite material on the support. On top, cross-section of the membrane support with the three layers; on bottom, top view micrograph of the 0.2 µm-layer pore-plugged with zeolite crystals.

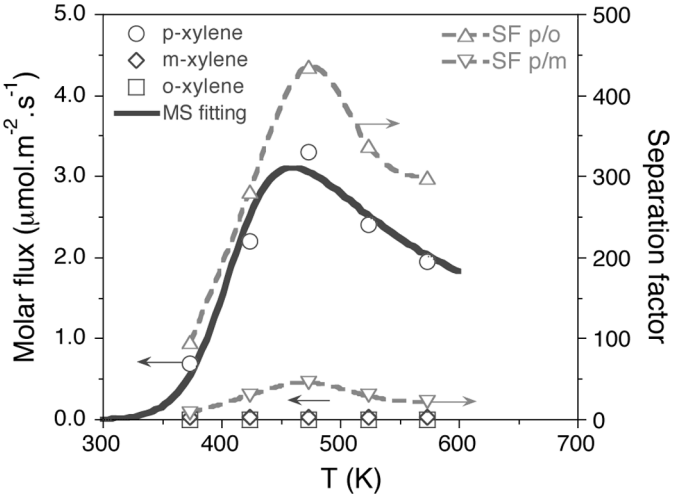

FIG. 3. Xylene ternary vapor mixture separation as a function of temperature within a nanocomposite MFI-alumina membrane. Experimental conditions: p-/m-/o-xylene feed partial pressures, 0.63 kPa/0.27 kPa/0.32 kPa; sweep gas flow rate, 15 mL (STP)/min; feed flow rate, 10 mL(STP)/min. The straight line corresponds to the MS fitting for p-xylene flux, while the dashed lines for separation factors are a guide to the eye.

at temperatures higher than 700 K. The temperature-dependence of the transmembrane p-xylene flux can be well represented by a pure gas Maxwell-Stefan (MS) adsorption-diffusion model under weak confinement (the MS surface diffusivity does not depend on the xylene loading) neglecting the influence of the other xylene isomers (Eq. 2)

$$N = \frac{c_{sat}\rho\varepsilon D_0(T)}{\tau\ell} Ln\left[\frac{1+K(T)P_R/P^o}{1+K(T)P_P/P^o}\right] \qquad (2)$$

with parameter values:

- R: ideal gas constant ($8.314\,J\cdot mol^{-1}\cdot K^{-1}$)
- ρ_{MFI}: MFI density ($1700\,kg\cdot m^{-3}$)
- ε: porosity of the nanocomposite MFI/alumina structure (0.13)
- c_{sat}: p-xylene loading at saturation ($0.25\,mol.kg^{-1}$ (33))
- $D_0(T_{ref})$: MS surface diffusivity at zero coverage at T_{ref} ($3.4\times10^{-13}\,m^2.s^{-1}$ at 473 K, value obtained with loading correction (29))
- τ: tortuosity (1.2)
- ℓ : effective MFI thickness (m, fitted parameter)
- P_R: retentate pressure [Pa]
- P_P: permeate pressure [Pa]
- P^o: reference to atmospheric pressure (101325 Pa)
- $K(T_{ref})$: adsorption constant of p-xylene on MFI at T_{ref} ($4.1\times10^{-4}\,Pa^{-1}$ at 473 K, value estimated from ref (31).)
- ΔH^0_{ads}: standard adsorption enthalpy ($-72000\,J\cdot mol^{-1}$ (33,35))
- E_D: diffusion activation energy ($J\cdot mol^{-1}$, fitted parameter)

A least-square non-linear optimization method, based on the Levenberg-Marquardt algorithm, was used to fit the zero-loading MS surface diffusivity at T_{ref} ($D_o(T_{ref})$) and the diffusion activation energy (E_D) by comparison of predicted and experimental p-xylene fluxes. In the fitting process, both parameters were expressed by an Arrhenius-type equation using, respectively, Eqs. 3 and 4.

$$K(T) = K(T_{ref})\left[-\frac{\Delta H^0_{ads}}{R}\left(\frac{1}{T}-\frac{1}{T_{ref}}\right)\right] \qquad (3)$$

$$D_0(T) = D_0(T_{ref})\left[-\frac{E_D}{R}\left(\frac{1}{T}-\frac{1}{T_{ref}}\right)\right] \quad (4)$$

where T_{ref} is the mean temperature of the series, in this case 473 K.

The values obtained for the fitted MFI effective thickness and activation energy for p-xylene diffusion are, respectively, $\ell = 0.83 \pm 0.04\,\mu m$ and $E_D = 60 \pm 2\,kJ \cdot mol^{-1}$. The latter value compares well with the value about $55\,kJ \cdot mol^{-1}$ measured by Masuda et al. (36) on H-ZSM-5 powders using the constant volume method, but is significantly higher than the value about 30 kJ/mol measured by Ruthven et al. (37) and Niessen et al. (38) on large silicalite single crystals.

The good prediction level of the MS model for the range of xylene total pressures considered here suggests that, as put forward by several authors (23,33), no relevant structural change of the MFI framework occurs upon p-xylene adsorption at temperatures higher than 373 K (the "critical" temperature). Moreover, as suggested by Hedlund in a very recent paper (39), the typical p-xylene adsorption pattern can be altered due to size effects when tuning from microsized to nanosized particles, the isotherm not showing the typical 2 steps (S-form) at low temperatures. The presence of MFI crystals of size <200 nm in a nanocomposite MFI-alumina membrane (the size of the support top layer), together with their strong confinement in the porous alumina network, might compensate the distorsion of the MFI framework upon p-xylene adsorption, avoiding the phase change traditionally observed for MFI powder at temperatures <400 K.

Effect of Sweep Gas Flow Rate

Figure 4 plots the effect of the sweep gas flow rate on the membrane permeation and separation performance in the separation of ternary p/m/o-xylene mixtures. As expected, the p-xylene flux increases with the N_2 flow rate up to a plateau value beyond 20 mL(STP)/min. This trend should be ascribed to a reduction of the p-xylene permeate partial pressure as the sweep gas flow rate increases. This might contribute to a decrease of the p-xylene surface coverage at the membrane/permeate surface and in its turn to an increase of the p-xylene driving force across the membrane. This trend is qualitatively predicted by the MS model (Eq. 3) using the parameters obtained from the fittings of p-xylene flux with temperature (see Fig. 3). The discrepancy between the experimental and predicted p-xylene fluxes at higher sweep gas flow rates can be partially attributed to a lack of accuracy in measuring p-xylene partial pressures at such conditions. The p/m and p/o separation factors show an increase with the sweep gas flow rate, reaching a value as high as 1000 (in practice infinite) at 473 K for sweep gas flow rates higher than 30 mL(STP)/min.

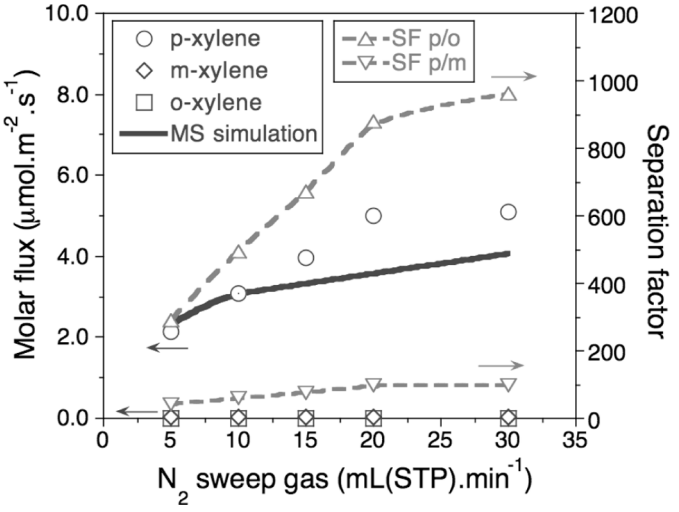

FIG. 4. Xylene ternary vapor mixture separation as a function of N_2 sweep gas flow rate within a nanocomposite MFI-alumina membrane. Experimental conditions: p-/m-/o-xylene feed partial pressures, 0.59 kPa/0.45 kPa/0.40 kPa; temperature, 473 K; feed flow rate, 10 mL (STP)/min. The straight line corresponds to the p-xylene flux predicted by Eq. 2, while the dashed lines for separation factors are a guide to the eye.

Effect of Xylene Feed Partial Pressure

Figure 5 shows the effect of the total xylene vapor pressure on the p/m/o xylene molar fluxes and the p/o and p/m xylene separation factors at 473 K (the temperature corresponding to the maximum flux). As can be seen, up

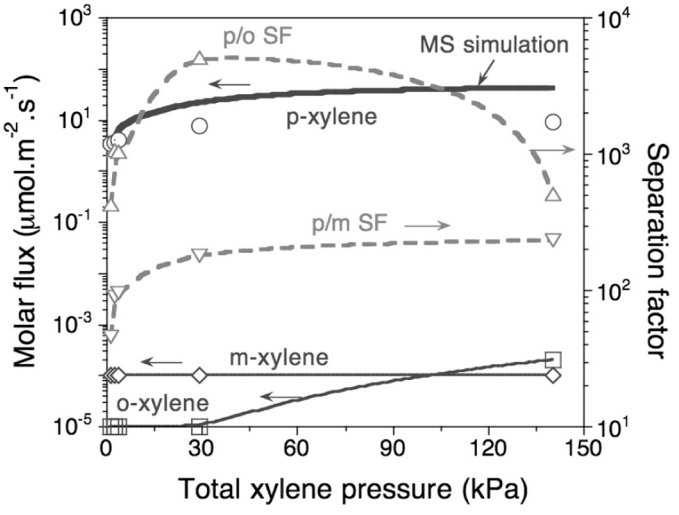

FIG. 5. Xylene ternary vapor mixture separation as a function of total xylene vapor pressure within a nanocomposite MFI-alumina membrane. Experimental conditions: p-/m-/o-xylene feed composition, 1:1:1 up to 15 kPa and 1:1:3 beyond 30 kPa; temperature, 473 K; feed flow rate, 10 mL(STP)/min, sweep flow rate, 15 mL(STP)/min. The straight and dashed lines, respectively, for xylene fluxes and separation factors are a guide to the eye.

to 150 kPa total xylene pressure, the p-xylene flux increases steadily with the total xylene vapor pressure for p/m/o-xylene equimolar mixtures up to 15 kPa and p/m/o xylene ratios of 1 : 1 : 3 beyond 30 kPa. In its turn, the permeance decreases steadily from 11 to 1 $\mu mol \cdot m^{-2} \cdot s^{-1} \cdot Pa^{-1}$. The p/m xylene separation factor remains practically invariable at a value of 200 with the xylene vapor pressure up to 150 kPa. In the case of the p/o xylene separation factor, after showing a maximum value about 5000 at 30-kPa xylene vapor pressure, it drops drastically to a value lower than 100 at 130 kPa.

The trend observed for the p-xylene flux should be attributed to the higher surface coverage of p-xylene and the retentate/membrane surface, enhancing therefore the p-xylene driving force across the membrane as predicted by the MS model (Eq. 3). At lower xylene partial pressures, keeping the xylene isomers at equimolar composition, selective adsorption of p-xylene on MFI blocks adsorption of other xylene isomers, thereby paving the way for them to permeate. At higher xylene vapor pressure, however, o-xylene adsorption becomes promoted, showing a slight permeation and contributing therefore to the observed decrease of the p/o xylene separation factor. This result seems to indicate that, at high xylene coverage, distortion of the MFI framework occurs, larger xylene isomers being able to be transfered within the MFI layer. At this juncture, taking into account the similar adsorption properties of the three xylene isomers on MFI zeolites, single-file diffusion can become promoted, the three isomers competing then for passage through the zeolite pores. As a result, the slower permeating isomers (i.e., m- and o-xylene) can reduce the permeance of the fastest one (p-xylene), the membrane selectivity being therefore drastically reduced. Moreover, as put forward by O'Brien-Abraham et al. (40), sorbate-sorbate competition for passage within the MFI pores in xylene mixture vapor permeation might also reduce the accessibility of p-xylene to MFI channels, hindering therefore its permeation.

Role of MFI Confinement on the Xylene Vapor Permeation Performance

Unlike film-like membranes, where the membrane selectivity is strongly affected by the xylene vapor pressure, the membranes prepared in this study still exhibit high p/o and p/m separation factors for xylene pressures as high as 150 kPa and for a p/m/o ratio of 1:1:3. The improved selective character of the membranes prepared in this work should be attributed to their nanocomposite architecture, minimizing long term stresses and in its turn the distortion of the MFI framework at high xylene loadings. Note that the same property of nanocomposite materials enable them to avoid crystal opening at high temperature due to thermal expansion mismatch between MFI crystals and the alumina support.

The high p-xylene separation performance of the membranes prepared in this study opens up a possible application of these materials to carry out xylene separation by PV, involving high xylene loadings. As far as we know, only Lin and Yang (9) have reported on the preparation of MFI membranes (without template and using seeded hydrothermal synthesis) for p-xylene separation. Their results show a p/o selectivity of 60 at 323 K in the separation of an equimolar p/o xylene binary mixture.

CONCLUSIONS

The results presented in this paper prove the excellent xylene separation performance of nanocomposite MFI-alumina membranes at high xylene loadings and high m- and o-xylene compositions. The intimate contact of alumina and the MFI nanoparticles at the nanoscale allows compensation of long-term stresses, attenuating the distortion of the MFI framework upon xylene adsorption. This property of nanocomposite MFI-alumina membranes is outstanding, since, unlike their film-like counterparts, the membranes can be operated at higher xylene vapor pressures without showing a dramatic decrease of their selectivity.

Furthermore, the hydrodynamics at the permeate side of the membranes plays a relevant role in their permeation and separation performance. As a matter of fact, the increase of turbulence in the permeate allows a drastic reduction of xylene partial pressures, promoting therefore permeation fluxes and selectivity to p-xylene. It is also highly expected, although not reported in this paper, that the application of a vacuum on the permeate side would improve the permeation and separation performance.

ACKNOWLEDGEMENTS

The authors hereby acknowledge the financial assistance of the French Embassy in Pretoria and the CNRS (France) and the NSF (South Africa) for funding this work through the PICS joint program. The authors thank Dr. A. Alshebani for his assistance in the preparation of the MFI membrane.

REFERENCES

1. Smitha, B.; Suhanya, D.; Sridhar, S.; Ramakrishna, M. (2004) Separation of organic mixtures by pervaporation—a review. *J. Membr. Sci.*, *241*: 1–21.
2. The 6th European Aromatics & Derivatives Conference, 14–15 November2007,Antwerp,Belgium. (http://www.tecnon.co.uk/gen/z_sys_Products.aspx?productid=63 (accessed 19th February 2009).
3. Moore, S.K. (1991) Sorting out the prospects for novel separations. *Chemical Week*, *161* (44): 53.
4. Energy and Environmental Profile of the U.S. Chemical Industry May 2000. U.S. Department of Energy Office of Industrial Technologies. Energetic Inc., Columbia Maryland, 2000.
5. Fabri, J.; Graeser, U.; Simo, T.A. (2002) *Xylene in Ullmann's Encyclopedia of Industrial Chemistry*, 7th Ed.; John Wiley & Sons, Inc., 2009.
6. Xylenes, Publication Details. Nexant Chem Systems. 01-May 02.http://nexant.ecnext.com/coms2/summary_0255-114_ITM.

7. Buchaly, C.; Kreis, P.; Gorak, A. (2007) Hybrid separation processes: Combination of reactive distillations with membrane separation. *Chem. Eng. Process*, *46*: 112.
8. Stephan, W.; Noble, R.D.; Koval, C.A. (1995) Design methodology for a membrane/distillation column hybrid process. *J. Membr. Sci.*, *99*: 259–272.
9. Yuan, W.; Lin, Y.S.; Yang, W. (2004) Molecular sieving MFI-type zeolite membranes for pervaporation separation of xylene isomers. *J. Am. Chem. Soc.*, *126*: 4776–4777.
10. Baetsch, C.D.; Funke, H.H.; Falconer, J.L.; Noble, R.D. (1996) Permeation of aromatic hydrocarbon vapors through silicalite-zeolite membranes. *J. Phys. Chem.*, *100*: 7676–7679.
11. Keizer, K.; Burggraaf, A.J.; Vroon, Z.A.E.P.; Verweij, H. (1998) Two-component permeation through thin zeolite MFI membranes. *J. Membr. Sci.*, *147*: 159–172.
12. Matsufuji, T.; Nishiyama, N.; Matsukata, M.; Ueyama, K. (2000) Separation of butane and xylene isomers with MFI-type zeolitic membrane synthesized by a vapor-phase transport method. *J. Membr. Sci.*, *178*: 25–34.
13. Gump, C.J.; Tuan, V.A.; Noble, R.D.; Falconer, J.L. (2001) Aromatic permeation through crystalline molecular sieve membranes. *Ind. Eng. Chem. Res.*, *40*: 565–577.
14. Sakai, H.; Tomita, T.; Takahashi, T. (2001) P-xylene separation with MFI-type zeolite membrane. *Sep. Purif. Technol.*, *25*: 297–306.
15. Hedlund, J.; Jareman, F.; Bons, A.J.; Anthonis, M. (2003) A masking technique for high quality MFI membranes. *J. Memb. Sci.*, *222*: 163–179.
16. Hedlund, J.; Sterte, J.; Anthonis, M.; Bons, A.J.; Carstensen, B.; Corcoran, N.; Cox, D.; Deckman, H.; De Gijnsr, W.; de Moor, P.-P.; Lai, F.; McHenry, J.; Mortier, W.; Reinoso, J.; Peters, J. (2002) High-flux MFI membranes. *Micropor. Mesopor. Mater.*, *52*: 179.
17. Gu, X.; Dong, J.; Nenoff, T.M.; Ozokwelu, D.E. (2006) Separation of p-xylene from multicomponent vapor mixture using tubular MFI zolite membranes. *J. Membr. Sci.*, *280*: 624–633.
18. Tarditi, A.M.; Horowitz, G.I.; Lombardo, E.A. (2006) A durable ZSM-5/SS composite tubular membrane for the selective separation of p-xylene from its isomers. *J. Membr. Sci.*, *281*: 692–699.
19. Flanigen, E.M.; Bennett, J.M.; Grose, R.W.; Cohen, J.P.; Patton, R.L.; Kirchner, R.M. (1978) Silicalite, a new hydrophobic crystalline silica molecular sieve. *Nature*, *271*: 512.
20. Choudhary, V.R.; Nayak, V.S.; Choudhary, T.V. (1997) Single-component sorption/diffusion of cyclic compounds from their bulk liquid phase in H-ZSM-5 zeolite. *Ind. Eng. Chem. Res.*, *36*: 1812–1818.
21. Mentzen, B.F.; Gelin, P. (1995) The silicalite/p-xylene system: Part I – Flexibility of the MFI framework and sorption mechanism observed during p-xylene pore-filling by X-ray power diffraction at room temperature. *Mater. Res. Bull.*, *30*: 373–380.
22. Mohanty, S.; Davis, H.T.; McCormick, A.V. (2000) Shape selective adsorption in atomistic nanopores: study of xylene isomers in silicalite. *Chem. Eng. Sci.*, *55*: 2779–2792.
23. Xomeritakis, G.; Nair, S.; Tsapatsis, M. (2000) Transport properties of alumina-supported MFI membranes made by secondary (seeded) growth. *Micropor. Mesopor. Mater.*, *38*: 61–73.
24. Olson, D.H.; Kokotailo, G.T.; Lawton, S.L.; Meier, W.M. (1981) Crystal structure and structure-related properties of ZSM-5. *J. Phys. Chem.*, *85*: 2238–2243.
25. Lai, Z.; Bonilla, G.; Diaz, I.; Nery, J.G.; Sujaoti, K.; Amat, M.A.; Kokkoli, E.; Terasaki, O.; Thompson, R.W.; Tsapatsis, M.; Vlachos, D.G. (2003) Microstructural optimization of a zeolite membrane for organic vapor separation. *Science*, *300*: 456–460.
26. Van Dyk, L.; Lorenzen, L.; Miachon, S.; Dalmon, J.-A. (2005) Xylene isomerization in an extractor type catalytic membrane reactor. *Catal. Today*, *104*: 274.
27. Daramola, M.O.; Burger, A.J.; Pera-Titus, M.; Giroir-Fendler, A.; Lorenzen, L.; Miachon, S.; Dalmon, J.-A. (2009) Nanocomposite MFI hollow-fibre membranes via pore-plugging synthesis: prospects for xylene isomer separation. *J. Membr. Sci.*, *337*: 106–112.
28. Giroir-Fendler, A.; Peureux, J.; Mozzanega, H.; Dalmon, J.-A. (1996) Characterisation of a zeolite membrane for catalytic membrane reactor application. *Stud. Surf. Sci. Catal.*, *101A*: 127.
29. Miachon, S.; Landrivon, E.; Aouine, M.; Sun, Y.; Kumakiri, I.; Li, Y.; Pachtova Prokopova, O.; Guilhaume, N.; Giroir-Fendler, A.; Mozzanega, H.; Dalmon, J.-A. (2006) Nanocomposite MFI-alumina membranes via pore-plugging synthesis: preparation and morphological characterization. *J. Membr. Sci.*, *281*: 228–238.
30. Pachtová, O.; Kumakiri, I.; Kocirik, M.; Miachon, S.; Dalmon, J.-A. (2003) Dynamic desorption of adsorbing species under cross membrane pressure difference: A new defect characterisation approach in zeolite. *J. Membr. Sci.*, *226*: 101–110.
31. Alshebani, A.; Pera-Titus, M.; Yeung, K.L.; Miachon, S.; Dalmon, J.-A. (2008) Influence of desorption conditions before gas separation studies in nanocomposite MFI-alumina membranes. *J. Memb. Sci.*, *314*: 143–151.
32. Miachon, S.; Ciavarella, P.; van Dyk, L.; Kumakiri, I.; Fiaty, K. (2007) Nanocomposite MFI-alumina membranes via pore-plugging synthesis: Specific transport and separation properties. *J. Memb Sci.*, *298*: 71–79.
33. Talu, O.; Guo, C.J.; Hay, D.T. (1989) Heterogeneous adsorption equilibria with. *J. Phys. Chem.*, *93*: 7294–7298.
34. Brandani, S.; Jama, M.; Ruthven, D. (2000) Diffusion, self-diffusion and counter-diffusion of benzene and p-xylene in silicalite. *Micropor. Mesopor. Mater.*, *35–36*: 283–300.
35. Li, J.; Talu, O. (1993) Structural effect on molecular simulations of tight-pore systems. *J. Chem. Soc. Faraday Trans.*, *89*: 1683–1687.
36. Masuda, T.; Fujikata, Y.; Nishida, T.; Hashimoto, K. (1998) The influence of acid sites on intracrystalline diffusivities within MFI-type zeolites. *Micropor. Mesopor. Mater.*, *23*: 157–167.
37. Ruthven, D.M.; Eic, M.; Richard, E. (1991) Diffusion of C8 aromatic hydrocarbons in silicalite. *Zeolites*, *11*: 647–653.
38. Niessen, W.; Karge, H.G. (1993) Diffusion of p-xylene in single and binary systems in zeolites investigated by FTIR spectroscopy. *Micropor. Mater.*, *1*: 1–8.
39. Grahn, M.; Holmgren, A.; Hedlund, J. (2008) Adsorption of n-hexane in thin silicalite-1 films studied by FTIR/ATR spectroscopy. *J. Phys. Chem. C*, *112*: 7717–7724.
40. O'Brien-Abraham, J.; Kanezashi, M.; Lin, Y.S. (2008) Effects of adsorption-induced microstructural changes on separation of xylene isomers through MFI-type zeolite membranes. *J. Membr. Sci.*, *320*: 505–513.